Effect of Different Axle Configurations on Fatigue Life of Asphalt Concrete Mixture

Karim Chatti and Chadi S. El Mohtar

The fatigue life of an asphalt mixture under different truck axle configurations was determined directly from the indirect tensile cyclic load test by using load pulses that were equivalent to the passage of an entire axle group or truck. The dissipated energy approach was adopted in analyzing the results and determining the number of repetitions to failure for each case; a unique fatigue curve that can be used for multiaxle configurations was developed. Trucks consisting of up to 11 axles and axle groups of up to 8 axles were studied. The results indicated that the normalized damage per load carried decreased with an increasing number of axles within an axle group. Additionally, the fatigue lives predicted by using single load pulses were compared with the measured ones from the different axle groups and trucks.

Most fatigue tests on asphalt-based mixes are performed under single pulse loads or continuous sinusoidal loading. However, in the field, the pavement is subjected to different axle configurations, causing multiple pulse loading within a passage of a single axle group, with the shape of the pulse being a function of axle spacing, pavement structure, vehicle speed, and so forth. To determine the fatigue life under multiple axles, Miner's hypothesis is commonly applied to accumulate the damage resulting from the different axles within an axle group. This relation is given by Equation 1.

$$\frac{n_1}{N_{1f}} + \frac{n_2}{N_{2f}} + \frac{n_3}{N_{3f}} + \cdots + \frac{n_i}{N_{if}} + \cdots \le 1 \tag{1}$$

where

- i = ith level of applied strain–stress at point under consideration,
- n_i = actual number of applications at strain level i that is anticipated, and
- N_{if} = number of applications at strain level i expected to cause fatigue failure if applied separately.

Typically, the damage is calculated by using either the peak strains from all pulses or the peak of the first pulse and the intermediate strains (difference between peaks and valleys) within a multiple strain pulse (*1–3*).

In this paper, the fatigue response of an asphalt mixture was studied by using multiple pulse loadings within a cycle, simulating different axle configurations. The dissipated energy approach was used to analyze the test results, and a unique fatigue curve was established. This curve was shown to describe the fatigue response due to any axle configuration regardless of axle spacing, interaction level, and rest period. The fatigue lives, corresponding to various axle configurations and truck types, determined by using the dissipated energy-based fatigue curve, were then compared.

RESEARCH OBJECTIVE

The objective of the research described here was to investigate the effect of different axle configurations and truck types on the fatigue response of an asphalt mixture by laboratory testing and the dissipated energy approach.

INDIRECT TENSILE CYCLIC LOAD TEST

The indirect tensile test is conducted by applying a vertical compressive strip load on a cylindrical specimen. The load is distributed over the thickness of the specimen through two loading strips at the top and bottom, as indicated in Figure 1*a*. The strips are curved and have a radius equal to that of the specimen to ensure full contact over the entire seating area. All specimens tested were 4 in. in diameter and 2.5 in. thick, with a 0.5-in.-wide loading strip. This combination of specimen geometry and boundary conditions induces tensile and compressive stresses along both the vertical and the horizontal diameters, as indicated in Figure 1*b*. The tensile stresses, developed perpendicular to the direction of the load, have a relatively constant value over a large portion of the vertical diameter. This would result in failure of the specimen by splitting along the vertical diameter, as indicated in Figure 1*a*. Under high vertical loads, local shear failure may occur near the loading strips. In this research, care was taken to prevent this mode of failure and to ensure that the specimen failed in fatigue with cracking initiating at the center.

Five linear variable differential transformers (LVDTs) were used to measure the response of the specimen: four in the horizontal direction (two along the thickness of the specimen and two along the diameter of the specimen) and one used to monitor the vertical deformation, as indicated in Figure 2. The analytical formulations to calculate the stresses and strains at the center of the specimen are well known and can be found elsewhere (*4–6*). The strains at the center of the specimen can be calculated directly as a function of the measured deformations.

DISSIPATED ENERGY DENSITY AND FATIGUE FAILURE CRITERION

Dissipated Energy Density

Several researchers have proposed using dissipated energy to predict the fatigue life of asphalt mixtures (*2, 7–10*). Dissipated energy density is defined as the area within a stress–strain hysteresis loop

Department of Civil and Environmental Engineering, Michigan State University, 3546 Engineering Building, East Lansing, MI 48824.

(a)

FIGURE 2   LVDT configurations for indirect
tensile cyclic load.

1.   Under cyclic loading, a given strain level, ϵ_0, corresponds to a dissipated energy density, w_0 (equal to the area within the stress–strain hysteresis loop) (Figure 3*a*) and

2.   Under a strength test, the stored energy until cracking (SEC) is equal to the area under the stress–strain curve up to its peak stress (Figure 3*b*).

To determine the fatigue life of asphalt mix specimens from laboratory testing, it is necessary to decide on a fatigue failure criterion. Different failure criteria result in different numbers of load repetitions until failure. The most common failure criterion is the 50% reduction in the modulus, where failure is defined as the cycle at which the modulus value is half the initial value. An alternative approach is to use the energy concept to link fatigue and strength testing and to define fatigue failure.

Such a fatigue failure criterion can be defined by equating the cumulative dissipated energy density under cyclic loading to the SEC value obtained from a strength test. This criterion can be applied to any test type (e.g., flexural, tension, indirect tension tests) provided the fatigue and strength tests are conducted with the same test setup. For example, if one were to extend this criterion to flexural beam testing, then the SEC value would be the flexural strength obtained by loading a beam to failure under a constant rate of deformation.

Typically, the dissipated energy density remains constant and then starts increasing until the point of failure. The point at which the dissipated energy density starts increasing can be interpreted as the initiation of failure, and the corresponding cycle number could be the number of load repetitions to crack initiation.

Figure 4*a* shows the N_f value using the dissipated energy density per cycle plot. The shaded area bounded by N_f corresponds to SEC. Figure 4*b* presents the SEC value plotted on the cumulative dissipated energy density curve. The intersection of the SEC line with the cumulative dissipated energy density curve is the fatigue life (N_f). The validity of the failure criterion is shown by using the fatigue test results described in the following section.

(b)

FIGURE 1   Indirect tensile test: (*a*) indirect tensile loading and
(*b*) stresses in the indirect tensile test specimen.

LABORATORY FATIGUE TESTING

under cyclic loading and represents the energy lost at a specific point due to a load application. In this paper, the tensile stresses and strains at the center of an indirect tensile specimen are used to calculate the dissipated energy density.

The asphalt mix used in this study was a 4E3 Superpave® mix with a top aggregate size of $\frac{1}{2}$ in. and a target asphalt content of 5.9%. The mix was obtained from an actual batch that was produced in a

Fatigue Failure Criterion

It is well known that for portland cement concrete mixes, fatigue curves are defined in terms of the stress ratio, σ/MR, where σ is the applied cyclic bending stress and *MR* is the modulus of rupture determined from a flexural strength test. The main advantage of this concept is that it links fatigue testing to a simple strength test.

For flexible pavement design, the strain level and the asphalt mix stiffness are used instead in the fatigue relationship. The concept of relating fatigue test results to a simple strength test is appealing because of the simplicity of such a test and because it characterizes the mixture. Because the strain level is important in fatigue testing of asphalt mixtures, a good way to relate fatigue testing to a strength test would be with energy. The energy density is defined as the product of stress and strain, so that
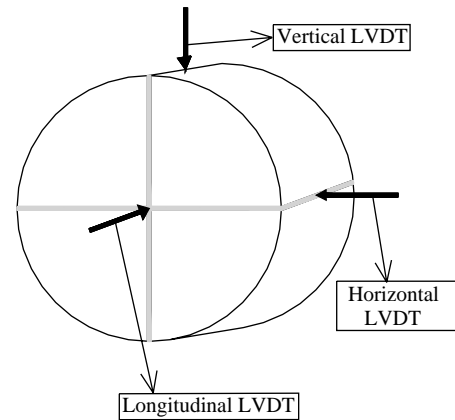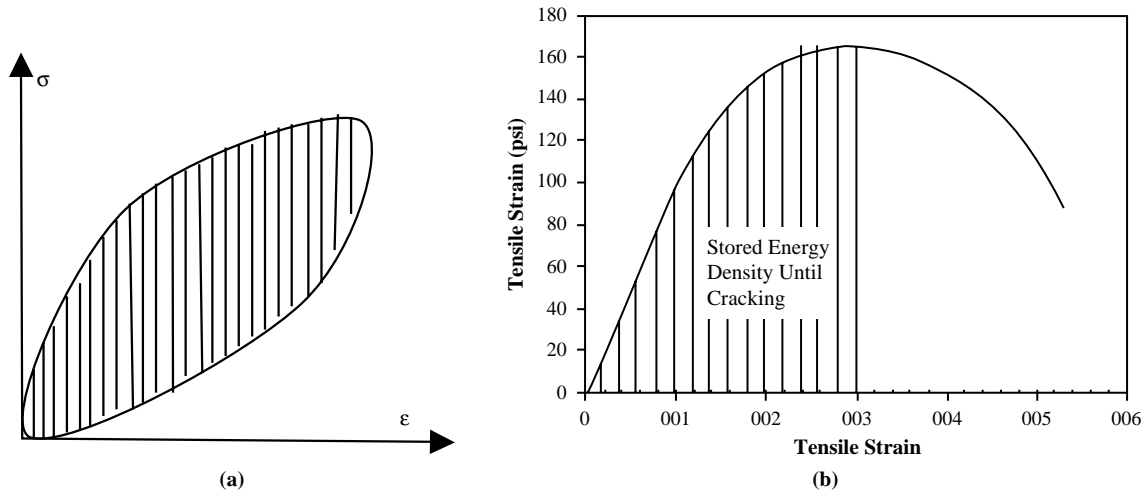
FIGURE 3   Stress–strain relationships under cyclic load and strength testing: (*a*) dissipated energy density under cyclic load testing and (*b*) stored energy density until failure under strength testing.
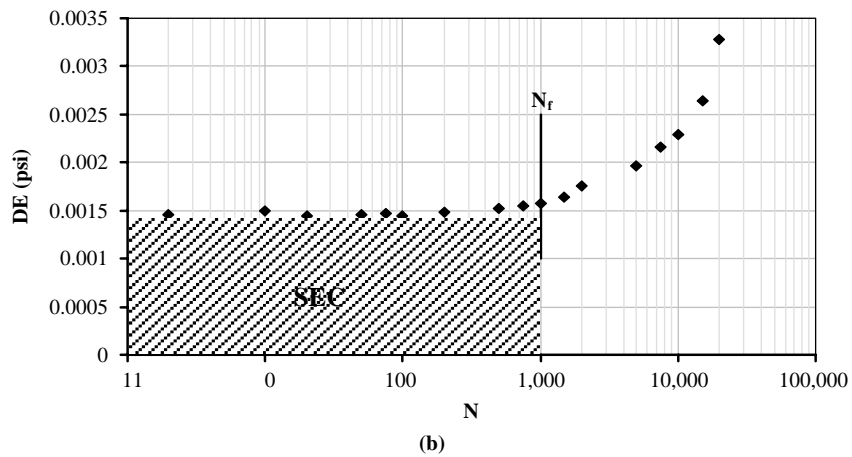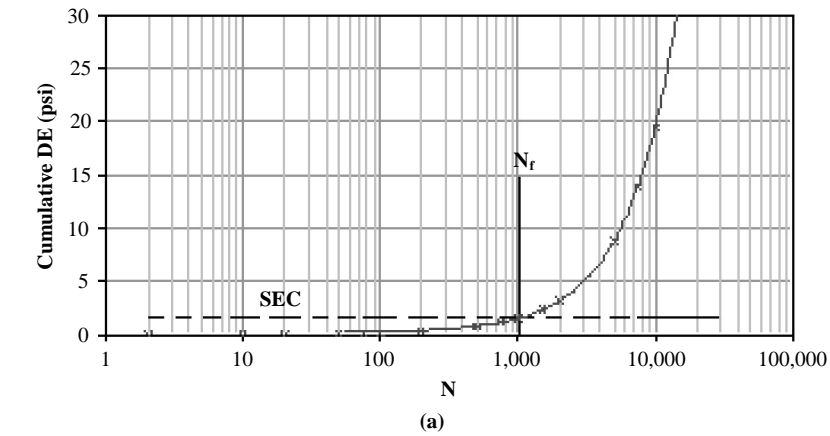

FIGURE 4   Fatigue failure criteria: (*a*) determining N_f from cumulative dissipated energy (DE) density and SEC and (*b*) determining N_f from dissipated energy density per cycle and SEC.

TABLE 1   Volumetric Properties of Mix

Property	G_{mm}	G_{mb}	G_{se}	G_{sb}	VMA	VFA	G_b
Value	2.487	2.388	2.731	2.661	15.6%	74.4%	1.026

NOTE: G_{mm} = maximum theoretical specific gravity of the mix, G_{mb} = bulk specific gravity of the mix, G_{se} = effective specific gravity of the aggregate, G_{sb} = bulk specific gravity of the aggregate, VMA = voids in mineral aggregate, VFA = voids filled with asphalt, G_b = specific gravity of the binder (asphalt).

mixing plant and used by the Michigan Department of Transportation on a project in the summer of 2002. The volumetric properties of the mix are presented in Table 1.

Fifty-seven samples (4 in. in diameter) were compacted in the laboratory with the gyratory compactor. The average air voids content was 3.9% and the standard deviation was 0.2%. Because specimens with high or low air voids were not tested, the total number of specimens used in the experiment equaled 47. Thirty-five specimens were tested for fatigue; three samples were tested under the indirect tensile strength test to determine the indirect tensile strength, and three more samples were tested under the indirect tensile strength test with horizontal deformation measurements to determine SEC. Three samples were tested for resilient modulus; three were tested under cyclic loading to determine the initial dissipated energy under various axle configurations. All testing was done at room temperature, with the average temperature recorded at about 70°F.

The average tensile strength was 171 psi, with the lowest and highest values being 168 and 174 psi, respectively. The average stored energy density until failure was 1.556 psi with the lowest and highest values being 1.547 and 1.568 psi, respectively. The average resilient modulus was 252,575 psi, and the standard deviation was 18,706 psi.

Thirty-one samples were tested for fatigue according to the test matrix presented in Table 2. Specimens were tested under different load pulses corresponding to five axle configurations—single, tandem, tridem, four axles, and eight axles—with each individual axle carrying a nominal load of 13 kips and with spacing between axles at 3.5 ft. In addition, two specimens were tested under continuous pulse loading (i.e., with no rest period), and two others were tested under a full truck with an 11-axle configuration—(one single axle, two tandem axles, and two tridem axles). The total number of fatigue tests equaled 35.

Three tensile stress levels were used: low, medium, and high. The medium stress level (8.75 psi) was determined by equating the horizontal (transverse) tensile strain at the bottom of a 6-in. asphalt concrete (AC) layer subjected to a 13-kip single axle load, as predicted by the SAPSI-M computer program (11), with the tensile strain at the center of the 4-in. specimen in the laboratory. The low and high stress levels (4.375 and 17.5 psi) were equal to half and double the medium stress level, respectively. The shape of the load pulse also was obtained by matching the tensile strain time histories at the bottom of the AC layer as predicted by SAPSI-M. Figure 5a presents an example of the strain time histories for a tridem axle, and Figure 5b presents a typical stress–strain hysteresis loop under a tridem load pulse. The ratio of loading–unloading duration to rest period was held constant at 1:4. For single axles, the loading–unloading duration was found to be 0.1 s by using the response calculated from SAPSI-M due to a load moving at 40 mph; therefore, a rest period of 0.4 s was used. For multiple axle configurations and trucks, the loading time was taken as the time from the beginning of the response due to the first axle until the time when the response of the axle dies, as calculated by SAPSI-M. Figure 6 presents examples of loading cycles used for fatigue testing. Three interaction levels were used for multiple axle groups: high, medium, and low. The interaction level is defined as the peak–valley stress ratio and represents different AC layer thicknesses (the thicker the AC, the higher the interaction level).

EXPERIMENTAL RESULTS

To verify the new failure criterion discussed previously, the number of cycles to failure, N_f, was determined with the new criterion as well as from visual inspection of the curve relating the dissipated energy per cycle to the number of load repetitions (for an example, see Figure 4). Figure 7a presents the relationship between N_f obtained by using SEC and that from visual inspection by using the dissipated energy density per cycle. The figure indicates that they are correlated, although there is large scatter. This is due to experimental error that makes it difficult to determine visually the number of cycles at which the dissipated energy density value starts to

TABLE 2   Experimental Fatigue Test Matrix

Stress Level	Axle no. / Interaction	1	2	3	4	8
Low	Low (25%)			x x		x x
	Medium (50%)	x x				
	High (75%)					
Medium	Low (25%)			x x x	x x x	x x x
	Medium (50%)	x x x	x x x			
	High (75%)					x x
High	Low (25%)		x x	x x		x x
	Medium (50%)	x x				
	High (75%)					

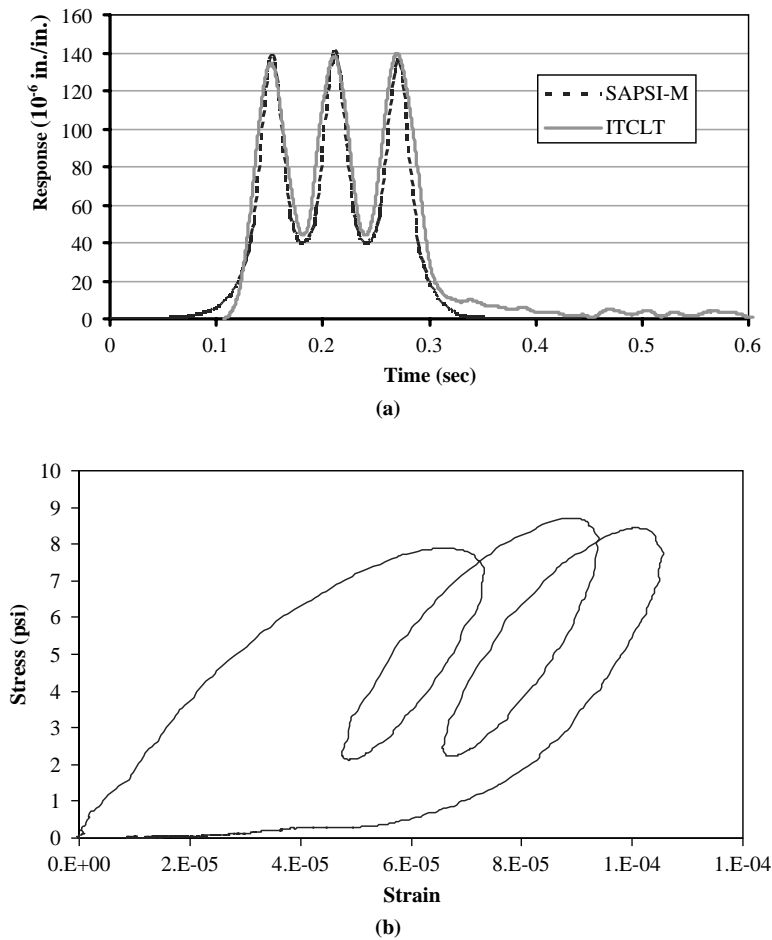No. of x's represents the number of samples tested.

FIGURE 5 Example strain and stress–strain response curves from cyclic load testing: (a) typical strain pulses from SAPSI-M and indirect tensile cyclic load test (ITCLT) results and (b) typical stress–strain hysteresis loop for tridem axle.

increase. This is confirmed by comparing the corresponding fatigue curves. Figure 7b presents the fatigue curve that is based on visual inspection; it shows a high degree of scatter. In contrast, Figure 8a presents the dissipated energy–based fatigue curve by using the new SEC criterion; the correlation has an R^2 value of 0.99. Clearly, this curve is unique and represents different axle configurations with different interaction and stress levels. Thus, using this fatigue curve would allow for determining the number of repetitions until failure for any axle configuration in one step without the need to build up an axle group from its components.

The fatigue model obtained is as follows:

$$N_f = 2.12 \ W_0^{-0.955} \tag{2}$$

where W_0 is initial dissipated energy density (psi).

Two samples were tested under a continuous (i.e., without rest period) haversine load at a medium stress level. Two more samples were tested under a load pulse simulating a whole truck. The truck used was an 11-axle Michigan truck (Truck 13 in Table 3). The whole truck was treated as one load cycle, and the dissipated energy density was calculated for passage of the whole truck. The rest period was determined on the basis of the same ratio used for the axle

groups (1 loading to 4 rest periods). The loading duration was taken from the point when the influence of the steering axle starts until the response due to the final axle dies. The results from continuous single pulse loading and truck loading were plotted on the same graph with the dissipated energy fatigue curve and are presented in Figure 8b. The points lie on top of the master dissipated energy–based fatigue curve and thus confirm its uniqueness. Therefore, no further fatigue testing was performed for other trucks or axle groups because the dissipated energy fatigue curve was found to be unique regardless of the load pulse. The procedure used to determine the damage factors for axle groups and trucks is presented next.

FATIGUE DAMAGE FACTORS FOR DIFFERENT AXLE GROUPS AND TRUCKS

In this section, the values of load equivalency factors (LEFs), truck factors (TFs), and axle factors (AFs) were determined by using the fatigue curve described previously. For a given axle group or truck configuration, LEF, TF, or AF was calculated from the fatigue curve by using the initial value of dissipated energy density corresponding to the passage of the entire axle group or truck. Some of the terms used in this analysis are defined next. LEF and TF are defined
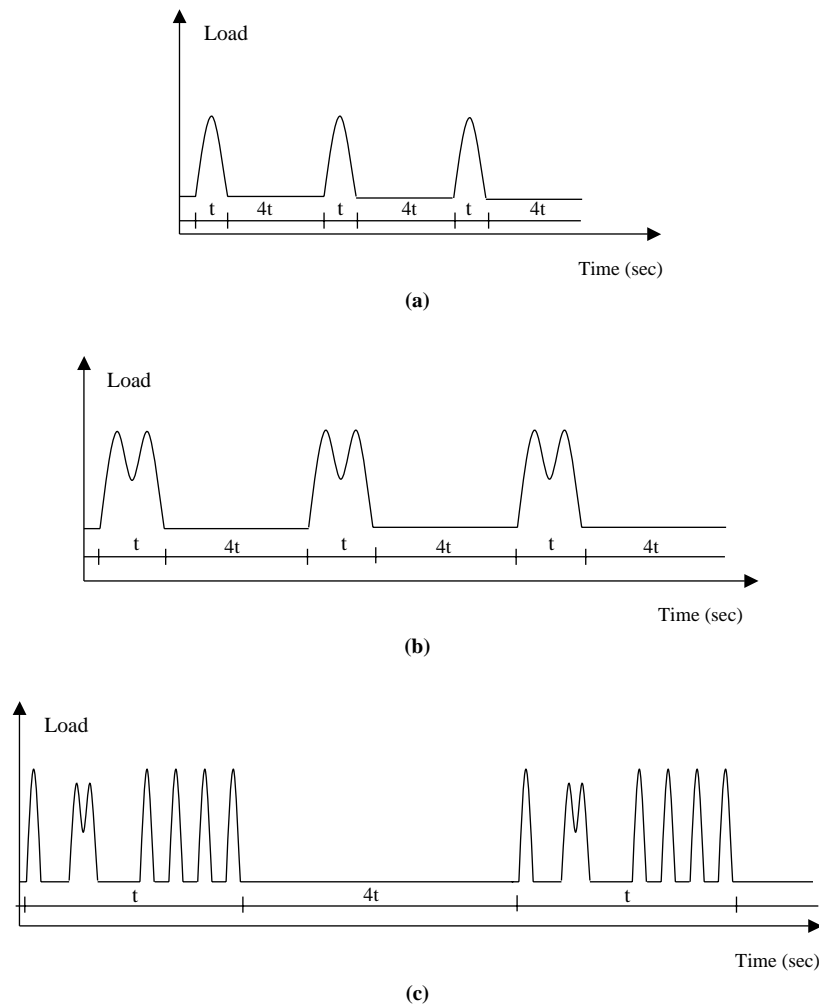
(a)

(b)

(c)

FIGURE 6   Examples of load cycles used in fatigue testing: (*a*) single axle, (*b*) tandem axle, and (*c*) Truck 10 (t is the duration of loading pulse and 4t is the rest period).

as the relative damage of an axle group or a truck to that of a standard axle, where damage is the inverse of the number of repetitions until failure.

$$
\text{LEF or TF} = \frac{\text{damage (axle configuration)}}{\text{damage (18-kip standard axle)}}
$$

$$
= \frac{N_f(\text{18-kip standard axle})}{N_f(\text{axle configuration})} \tag{3}
$$

AF is defined here as the relative damage of an axle group to that of a single axle carrying the same load as any of the axle group components. For example, the AF of a 39-kip tridem is determined as follows:

$$
\text{AF} = \frac{\text{damage (39-kip tridem)}}{\text{damage (13-kip single)}} = \frac{N_f(\text{13-kip single})}{N_f(\text{39-kip tridem})} \tag{4}
$$

LEF, AF, and TF per tonnage can be determined by dividing their respective values with the total load carried by the axle configuration. Using the per tonnage values allows for determining the most efficient axle configuration to carry a given payload.

The same specimen was used to determine the initial dissipated energy density for all axle groups and trucks studied, by using a limited number of load cycles and thus eliminating the variability of air voids content and the AC internal structure. Additionally, performing all the tests while the specimen was still in the same position in the loading frame decreased any errors due to specimen misalignment with the loading strips. Because the specimen was at the initial stage of the test, there was a negligible accumulated strain from subsequent load cycles. To verify this, the first axle configuration tested for initial dissipated energy on the specimen was again tested at the end of the test, and the corresponding dissipated energy was calculated to make sure it matched with the first value calculated at the beginning of the test. Trucks consisting of up to 11 axles and axle groups of up to 8 axles were studied. Ten trucks were selected for laboratory testing. The trucks were chosen to cover all axle configurations used in Michigan. Table 3 presents the truck configurations used. Three triplicates were used, and each load combination was applied for 15 cycles to determine the initial dissipated energy density. The results are presented in the following paragraphs.
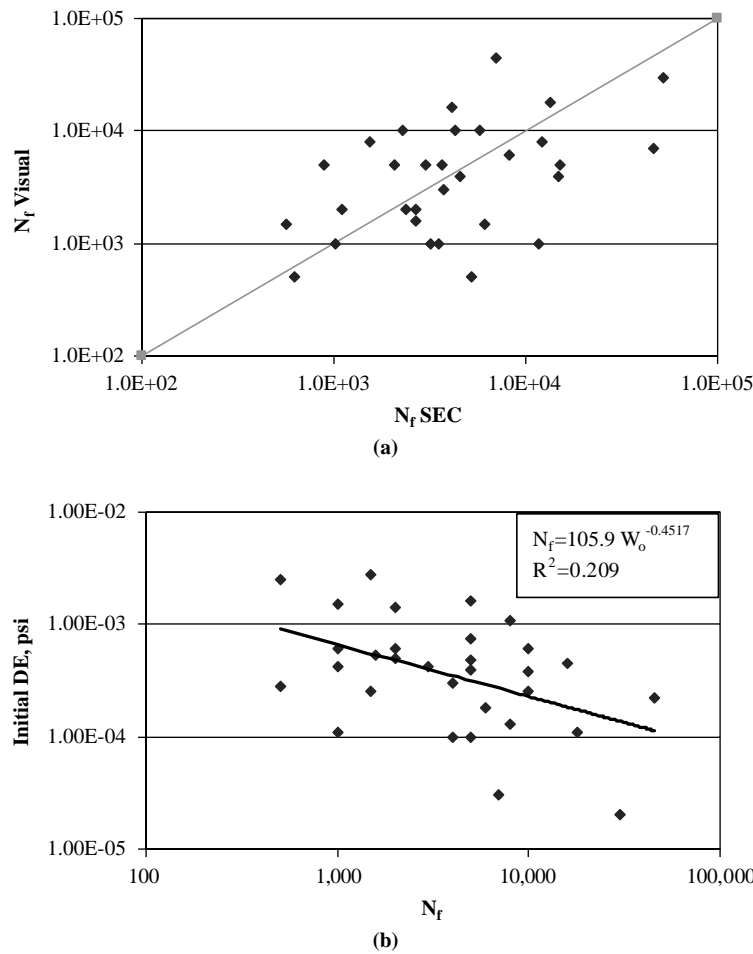
(a)

$$N_f = 105.9 \, W_o^{-0.4517}$$
$$R^2 = 0.209$$

(b)

FIGURE 7   Comparisons of visual and SEC failure criteria: (a) N_f based on visual criteria and SEC and (b) fatigue curve based on visual criteria (DE = dissipated energy).

Axle Fatigue Damage Factors

Table 4 presents the LEF and LEF per tonnage values for all axle groups studied, while Figure 9 presents the AF values per tonnage. The results confirm that using multiaxles to carry the same payload increases the fatigue life of an asphalt mix. The increase in fatigue life is much more significant when one goes from a single to tandem and tridem axles; the damage values per tonnage start to even out as the number of axles exceeds five. This implies that from a fatigue damage perspective, using an eight-axle configuration to carry 104 kips is much more beneficial than using eight separate axles carrying 13 kips each. The results also show that the effect of interaction level on the equivalent damage factors is not significant.

Truck Fatigue Damage Factors

The fatigue life corresponding to each truck was determined by using the dissipated energy fatigue curve, and the corresponding TF and TF per tonnage were calculated. Figure 10 presents the TFs per tonnage. The results show that Truck 1 is the most damaging per tonnage. Truck 1 is a two-axle single-body truck that consists of a 15.4-kip front steering axle and a single 18-kip standard axle in the rear. Trucks 13, 14, 17, 19, and 20 have the lowest TFs per tonnage because their payload is distributed over larger axle groups. The decrease in TF per tonnage from Truck 1 to Truck 4 emphasizes the same finding mentioned previously that multiaxle groups are less damaging than individual axles when one considers the load they carry. Truck 20, which has the most axles and least axle groups, is the most efficient of all trucks investigated.

CONCLUSION

On the basis of experimental results from fatigue testing of an AC mix under multiple axle configurations with the indirect tensile cyclic load test, the following conclusions are drawn:

1. The SEC failure criterion, developed in this study, was found to be a good failure criterion for fatigue life of AC mixes when the dissipated energy approach is used. This failure criterion indicates crack initiation in the specimen.
2. A unique energy-based fatigue curve developed for different axle and truck configurations is useful for predicting the fatigue life of an axle group or a truck at once without the need for summing up the damage from individual axles.
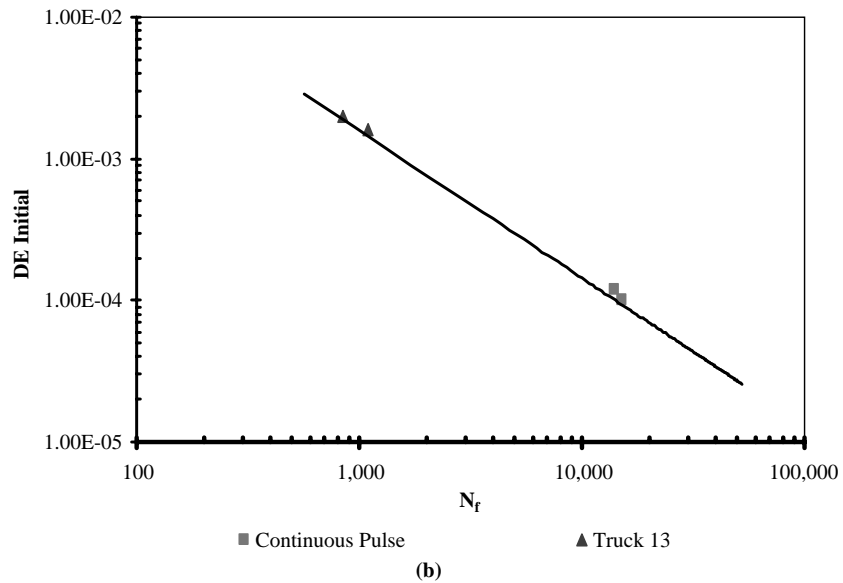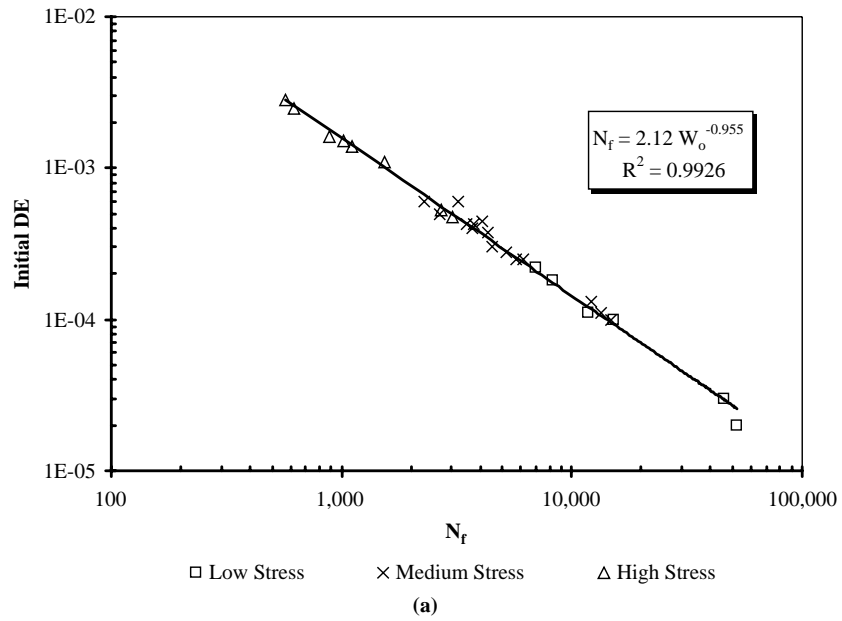
In plot (a):

$$N_f = 2.12\ W_o^{-0.955}$$
$$R^2 = 0.9926$$

□ Low Stress   × Medium Stress   △ High Stress

(a)

■ Continuous Pulse   ▲ Truck 13

(b)

FIGURE 8   Dissipated energy (DE)–based fatigue curve: (*a*) fatigue curve using various axle configurations and (*b*) fatigue responses under pulse load and truck.

TABLE 3 Truck Axle Configurations

Truck No.	No. of Axle Groups	No. of Axles	Truck Configuration
Truck 0	3	5	
Truck 1	2	2	
Truck 2	2	3	
Truck 3	2	4	
Truck 4	2	5	
Truck 10	6	7	
Truck 13	5	11	
Truck 14	6	11	
Truck 17	3	10	
Truck 19	3	10	
Truck 20	3	11	

TABLE 4 Summary of Results in Terms of Axle Load Equivalency Factors

N_f		N_f	LEF	LEF/Tonnage
1 axle 18-kip		5,388	1.00	1.00
1 axle 13-kip		7,750	0.70	0.96
25% Interaction	2 axles	4,889	1.10	0.76
	3 axles	3,876	1.39	0.64
	4 axles	2,889	1.87	0.65
	5 axles	2,377	2.27	0.63
	7 axles	1,893	2.85	0.56
	8 axles	1,707	3.16	0.55
50% Interaction	2 axles	5,987	0.90	0.62
	3 axles	4,592	1.17	0.54
	4 axles	3,577	1.51	0.52
	5 axles	2,992	1.80	0.50
	7 axles	2,477	2.18	0.43
	8 axles	2,289	2.35	0.41
75% Interaction	2 axles	5,644	0.95	0.66
	3 axles	4,155	1.30	0.60
	4 axles	3,431	1.57	0.54
	5 axles	3,058	1.76	0.49
	7 axles	2,549	2.11	0.42
	8 axles	2,439	2.21	0.38

$$y = 1.0043x^{-0.3363}$$
$$R^2 = 0.89$$

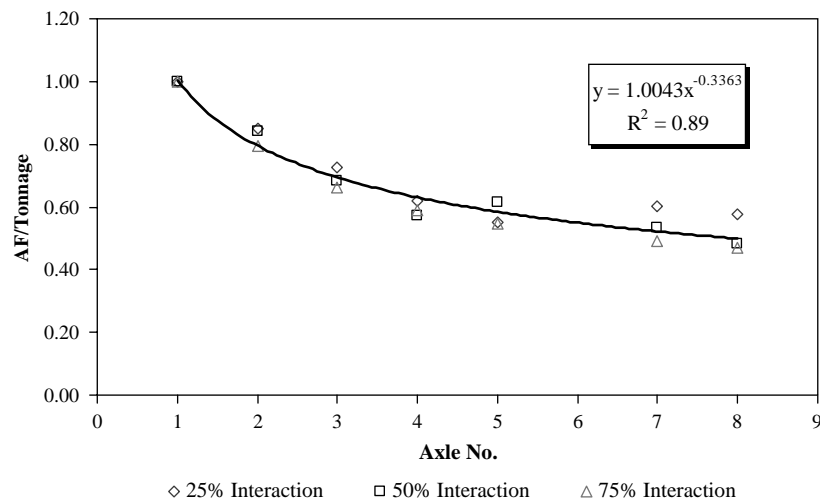◇ 25% Interaction   □ 50% Interaction   △ 75% Interaction

FIGURE 9   Axle factors per tonnage for different interaction levels.
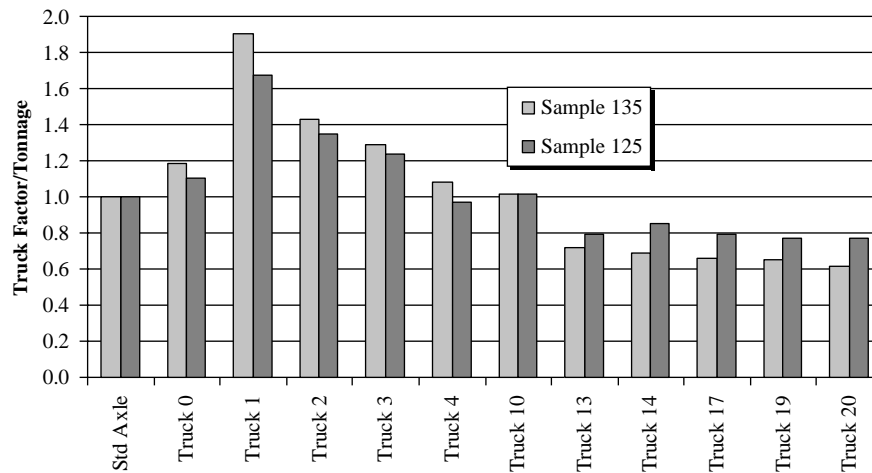
FIGURE 10   Truck factors per tonnage (Std = standard).

3. Multiple-axle groups were found to be less damaging per tonnage than single axles. Increasing the number of axles carrying the same load resulted in less damage. This decrease in damage was found to be more significant for single, tandem, and tridem axles, while it started to level off at higher axle numbers. Similar results were obtained for trucks, where trucks with more axles and axle groups had lower TFs per tonnage than those with single axles.

ACKNOWLEDGMENT

REFERENCES

1. Huang, H. Y. *Pavement Analysis and Design.* Prentice Hall, Englewood Cliffs, N.J., 1993.
2. Chatti, K., and H. S. Lee. Comparison of Mechanistic Fatigue Prediction Methods for Asphalt Pavements. *Proc., International Conference on Computational and Experimental Engineering and Sciences,* Corfu, Greece, July 24–29, 2003.
3. Hajek, J. J., and A. C. Agarwal. Influence of Axle Group Spacing on Pavement Damage. In *Transportation Research Record 1286,* TRB, National Research Council, Washington, D.C., 1990, pp. 138–149.
4. Baladi, G. Y. *Integrated Material and Structural Design Method for Flexible Pavements, Vol. 1. Technical Report.* FHWA-RD-88-109. FHWA, McLean, Va., 1988.
5. El Mohtar, C. *The Effect of Different Axle Configurations on the Fatigue Life of an Asphalt Concrete Mixture.* Master's thesis. Department of Civil and Environmental Engineering, Michigan State University, East Lansing, 2003.
6. Chatti, K., A. Iftikhar, and H. B. Kim. Comparison of Energy-Based Fatigue Curves for Asphalt Mixtures Using Cyclic Indirect Tensile and Flexural Tests. *Proc., 2nd International Conference on Engineering Materials,* 2001, pp. 271–282.
7. Van Dijk, W. Practical Fatigue Characterization of Bituminous Mixes. *Proc., Association of Asphalt Paving Technologists,* Vol. 44, 1975, pp. 38–74.
8. Van Dijk, W., and W. Visser. Energy Approach to Fatigue for Pavement Design. *Proc., Association of Asphalt Paving Technologists,* No. 46, 1977, pp. 1–40.
9. Sousa, J. B., G. Rowe, and A. A. Tayebali. Dissipated Energy and Fatigue of Asphalt Aggregate Mixtures. Presented at Annual Meeting of the Association of Asphalt Paving Technologists, University of California, Berkeley, Feb. 1992.
10. Ghuzlan, K. A., and S. H. Carpenter. Energy-Derived, Damage-Based Failure Criterion for Fatigue Testing. In *Transportation Research Record: Journal of the Transportation Research Board, No. 1723,* TRB, National Research Council, Washington, D.C., 2000, pp. 141–149.
11. Chatti, K., and K. K. Yun. SAPSI-M: Computer Program for Analyzing Asphalt Concrete Pavements Under Moving Arbitrary Loads. In *Transportation Research Record 1539,* TRB, National Research Council, Washington, D.C., 1996, pp. 88–95.